EFFECT OF CORE CUTTING TOPOLOGY AND MATERIAL OF THREE PHASE TRANSFORMER ON MAGNETIZATION CURVE AND INRUSH CURRENT: EXPERIMENTAL APPROACH

I Made Yulistya Negara[1], Daniar Fahmi[2], Dimas Anton Asfani[1], and Rahman Cahyadiputra[3]

[1] Department of Electrical Engineering, Institut Teknologi Sepuluh Nopember, Surabaya, Indonesia, e-mail: yulistya@ee.its.ac.id

[2] Department of Electrical Engineering, Institut Teknologi Sepuluh Nopember, Surabaya, Indonesia, e-mail: daniarfahmi.elits@gmail.com

[1] Department of Electrical Engineering, Institut Teknologi Sepuluh Nopember, Surabaya, Indonesia, e-mail: anton@ee.its.ac.id

[3] Department of Electrical Engineering, Institut Teknologi Sepuluh Nopember, Surabaya, Indonesia, e-mail: rahman11@mhs.ee.its.ac.id

Received Date: April 4, 2016

Abstract

This study conducts the core cutting topology effect in three phase transformer on magnetization curve and inrush current. Core cutting topology effect on magnetization curve and magnetic field is analyzed using Finite-Element Method (FEM) simulation at the points of connection between the core pieces. The magnetization curves are used to determine inrush current of each transformer. Therefore, calculated inrush current was then compared to experimental measurements of inrush currents. The existence of residual flux or remnant flux is considered in inrush current measurement, thus demagnetization method is used to obtain the real inrush current value. Simulation and experimental results show that the topology of the transformer core cutting affects the magnetization curves and inrush currents. These are proven by differences in the magnetization curve and inrush current of both topology transformer core cutting. It was also suggested that quality of core material affected the magnetization curve and inrush current.

Keywords: Core cutting topology, Core material, Inrush current, Magnetization curve, Three phase transformer

Introduction

Transformer is extremely important equipment in the electrical system. Transformer is used to increase or decrease voltage level so that electrical power can be used by electrical loads in homes, offices, and industry [1]. Protection system design related to the transformer needs to consider some the characteristics of the transformer phenomena. One of those phenomena is the inrush current. The phenomena of the transformer inrush current have been discussed in some literature [2-7]. Inrush current become consideration in design and protection performance of differential relay. That attention is influenced by the transformer energizing which magnetization current may be able to reach 10-20 times to rating current. Meanwhile, in steady state condition magnetization current only reach 1-2% of rating current [8].

The phenomenon of inrush current can be analyzed through the effect B-H curve on an iron core transformer [9]. B-H curve analysis on three phase transformer becomes a challenge because electromagnetic behavior in transient and steady state conditions are significantly different than the single phase transformer. Specifically more flux pathways and magnetic couplings on the three legs core show different behavior compared to the single transformer [10]. The air gap in the core and joint of core cutting part also affect

magnitude of magnetic saturation in transformer [11]. Analysis of the transformer core cutting effect on the curve magnetization and inrush currents using simulation software before shows the maximum magnetic field density and maximum magnetic field intensity in the magnetization curve is not proportional to the maximum inrush current. The study result also shows that there are differences in current value of the maximum inrush on a different transformer core cutting [12,13].

Therefore, in this study the effect of transformer core topology on inrush current is even further investigated. Study results from [13] will be verified using an experimental approach. The study procedures are similar with previous study besides of transformer rating. It begins from identification of common iron core cutting topology used in each transformer. Then FEM simulation method is performed to obtain magnetization curve thereupon inrush current can be determined. Similar transformer core topologies and rating are used in experimental setup so that it can be compared and analyzed with simulation result. Moreover, inrush current measurement comes with demagnetization techniques using shunt capacitor and Variable Voltage-Constant Frequency.

Transformer Principles

In simple terms, there are two types of transformer construction commonly used, such as the type of core-form and the type shell-form. At the core type coils are wound around two legs of a rectangular magnetic core. In core type construction each coil consists of two parts, the primary coil and the secondary coil are at different transformer leg. While on the shell-type construction coils are wound around the middle leg of the three leg core varied and not overlapping. On the shell-type construction, the primary and secondary windings can also be wound each other on one leg.

Non-Ideal Transformer

In practice, transformer cannot convert power perfectly. This is due to the effect of resistance coils, leakage fluxes, and excitation currents because of limited core permeability, even nonlinear. Not whole of fluxes generated pass through the secondary side. There are some parts of flux that does not pass into another coil but flowing freely into the air. Power losses due to core loss are affected by the resistance core and magnetic reactance occurs in the transformer core.

The limited permeability of magnetic circuit influences the magnitude of the current that be required to generate magnetic force to maintain transformer flux required in order to operate. The current and the magnetic force are proportional to the flux density (B) which occurs in the transformer core. This statement comes from

$$B = \mu H;\ B = \frac{\emptyset}{A} \tag{1}$$

where B is flux density, μ is permeability of core material, A is surface area of ferromagnetic core, $\emptyset$ is magnetic flux, and H is magnetizing force or magnetic field intensity. The value of H is obtained from

$$\mathrm{H} = \mathrm{i}\ \frac{T1}{l} \tag{2}$$

where l is length of magnetic path transformer core. So the influence of the magnetic path to magnitude of flux become,

$$\emptyset = \int B.dS = A\mu \frac{(iT1)}{l} \tag{3}$$

When the saturation conditions are considered in operation of non-ideal the transformer, the current is required to be adjusted with nonlinearity core to produce the voltage. The current is also affected by inductive reactance of the magnetization circuit. Thus the magnetization current is obtained from the applied voltage divided by the magnetization reactance. This magnetization circuit becomes losses that need to be considered because the circuit can dissipates power depending on the flux density work.

Through modeling the equivalent circuit of the non-ideal transformer, the winding and core parameters can be obtained. Furthermore, both of these parameters can be obtained using short-circuit and open-circuit tests of the transformer.

Transformer Inrush Current

When the AC power source is applied to the transformer for the first time, a current will flow into primary winding, even the secondary winding is not connected to the load. This current is called inrush current. This current is required to energize transformer for the first time to produce flux in the ferromagnetic core. This current is required till the maximum value of flux achieve steady state and the core becomes saturated.

Inrush currents occur in the transformer when the residual flux does not meet the instantaneous value of flux in steady state, especially at the specified voltage waveform points. Change rate of instantaneous flux in the transformer is proportional to an instantaneous voltage drop in the winding connected source. During energizing flux must begin at the zero point. Thus, to raise the voltage from zero, magnetic flux will reach a peak value much more than normal conditions. Due to nonlinearity characteristic of magnetization curve, on the saturated condition, the required magnetic moving force (mmf) is not linearly increasing to generate magnetic flux. It makes the coil current needed to create the mmf to cause the flux in the transformer core is also increasing more than normal condition. The phenomenon can be seen in Figure 1.

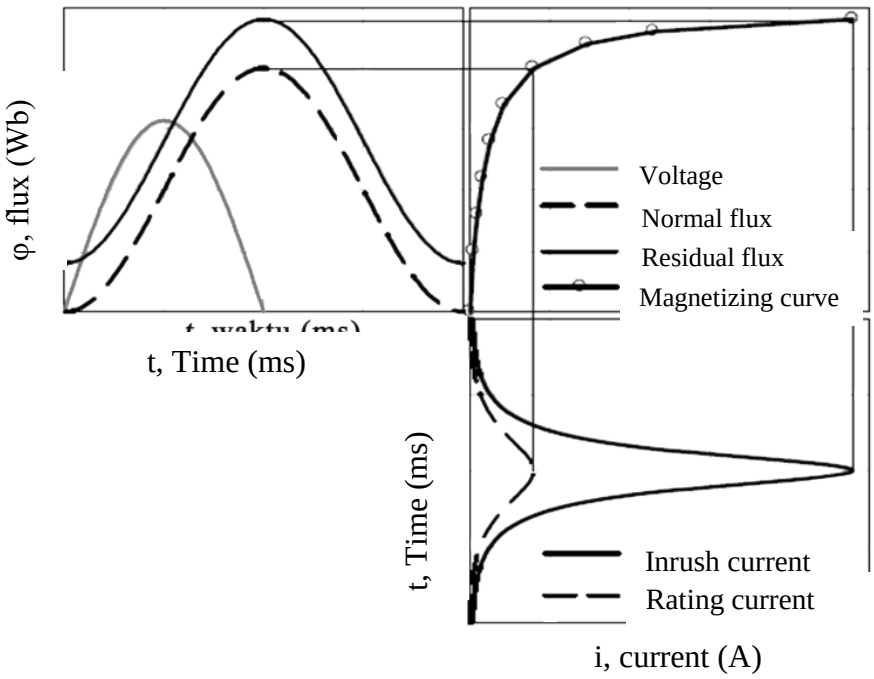

Figure 1. Relationship of inrush current with flux existence

Based on [14], inrush current peak value can be obtained using transformer parameters in operating condition. Mathematically, the value of inrush current can be determined using this equation,

$$i_{max} = \frac{\sqrt{2}Vm}{\sqrt{(\omega L)^2+R^2}}\left(\frac{2.Bn+Br+Bs}{Bn}\right) \quad (4)$$

where, Vm is maximum applied voltage, L is transformer inductance, R is transformer inductance, Bn is normal magnetic field density, Br is residual magnetic field density, and Bs is saturated magnetic field density of transformer.

Transformer Modeling Using Simulation of Finite - Element Method and Experimental Inrush Current Measurement

Specifications of Three Phase Transformers

The investigated transformers are three-phase transformer which has a different core cutting topology. There are 2 transformers with different core cutting topologies in comparison, namely the core cutting A and the core cutting B. The transformer core with the A cutting consists of 5 components formed by rectangular or letter I shape. While the transformer core with B cutting has 3 components, such as yoke, leg and center. General specifications of three-phase transformer can be seen in Table 1 and core cutting dimension can be seen in Table 2. Moreover, the shape of the three-phase transformer core cutting A can be seen in Figure 2 while B type can be seen in Figure 3.

Table 1. Specifications of Three Phase Transformer

Specification of Transformer	
Phase	3 Phase
Power Capacity	3000 VA
Primary Voltage	380 Volt
Secondary Voltage	380 Volt
Winding Connection	Y-Y
Number of Primary Winding	300
Number of Secondary Winding	300
Winding Resistance	0.024 Ohm / phase

Table 2. Cutting Dimension

Cutting Dimension	**Core Cutting A**	**Core Cutting B**
A	4 cm	21 cm
B	21 cm	21 cm
C	4.5 cm	13 cm
D	17 cm	4.5 cm
E	-	4 cm
Thickness	9 cm	9 cm

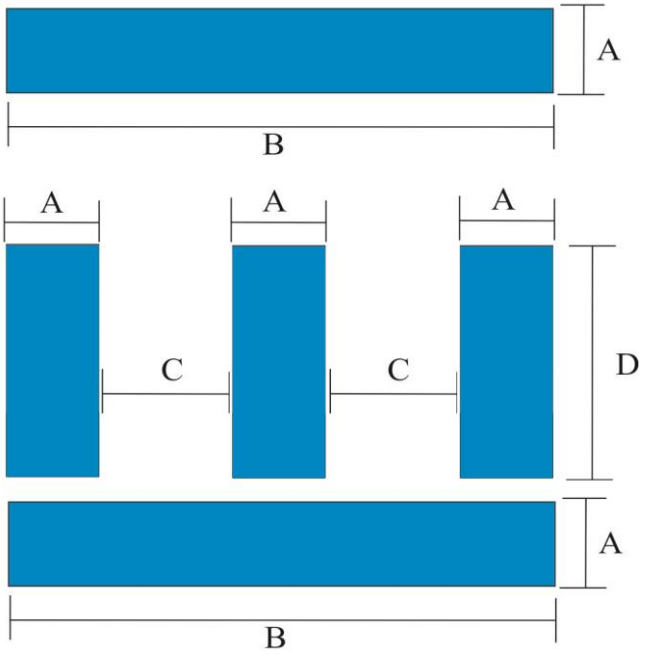

Figure 2. Three phase transformer core cutting of A type

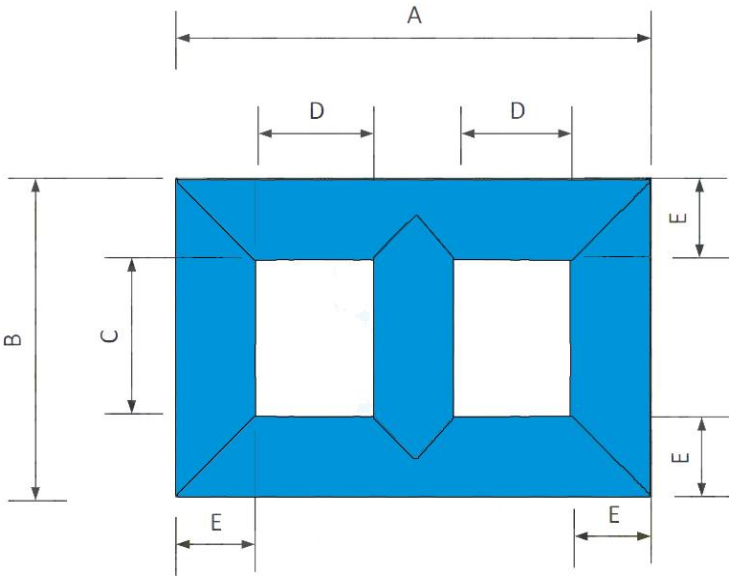

Figure 3. Three phase transformer core cutting of B type

Transformer Modelling Using Finite-Element Method (FEM)

Finite-Element Method is one of the numerical methods that can be used to solve the thermal, structural, and electromagnetic problem. FEM can be used to complete the three-dimensional computational elements by computing elements or subdomains that dimensional construct an object. Model transformer by designing the construction of three the dimensions of the transformer with FEM based software for core cutting A (El) and B (Yog Leg Center). The transformer models, then, computed use Finite-Element Method with mesh tetrahedron to find the value of B and H as seen in Figure 4. The total of mesh tetrahedrons is 21919 for cutting A with minimum and maximum edge length are 0.00745796 and 4.60964, respectively, and 14714 for cutting B with minimum and maximum edge length are 0.000751058 and 5.34638, respectively. However, both of them use the same material, st-37 with 7850 kg/m^3.

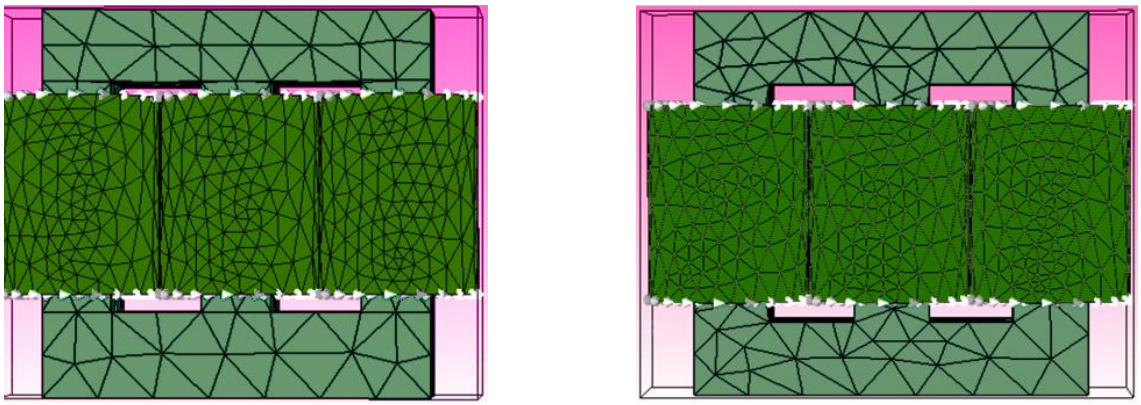

(a) (b)

Figure 4. Tetrahedral mesh construction of; core cutting A (a), core cutting B (b)

Equations for Electric Field Analysis

Since inrush current also correlates with electric field, it can be analyzed as Maxwell's equation (5) and Poisson's equation (6) below:

$$E = -\nabla V \tag{5}$$

$$\varepsilon \,.\, \nabla\,(\nabla\, V) = -\rho \tag{6}$$

If $\boldsymbol{\rho = 0}$ (without space charge), Poisson's equation becomes Laplace's equation:

$$\boldsymbol{\varepsilon \,.\, \nabla\,(\nabla\, V) = 0} \tag{7}$$

where ρ is resistivity Ω/m, ε is material dielectric constant ($\varepsilon = \varepsilon_0\varepsilon_r$), ε_0 is free space dielectric constant ($8.854x10^{-12}F/m$), and ε_r is relative dielectric constant of dielectric material.

Equations for Finite-Element Method (FEM)

Magnetization curve relate the density of the magnetic field, B, and the intensity of the magnetic field, H. This curve shows the effect of magnetic field density, B, which occurs at the core of the transformer due the increase in the intensity of the magnetic field H.

$$F(u) = \tfrac{1}{2}\textstyle\int_D \left[\varepsilon_x \left(\frac{du}{dx}\right)^2 + \varepsilon_y \left(\frac{du}{dy}\right)^2\right].dxdy \tag{8}$$

where ε_x and ε_r are $x-$ and $y-$component of dielectric constant in coordinates Cartesian system and u is the electric potential.

If ($\varepsilon = \varepsilon_x = \varepsilon_y$), equation (12) becomes:

$$F(u) = \tfrac{1}{2}\textstyle\int_D\ \varepsilon\left[\left(\frac{du}{dx}\right)^2 + \left(\frac{du}{dy}\right)^2\right].dxdy \tag{9}$$

Then, if the effect of dielectric loss is not negligible, equation (13) above can be rewritten as:

$$F(u^*) = \tfrac{1}{2}\textstyle\int_D\ \omega.\varepsilon_0.(\varepsilon - j\varepsilon.tg\delta)\left[\left(\frac{du^*}{dx}\right)^2 + \left(\frac{du^*}{dy}\right)^2\right].dxdy \tag{10}$$

where ω is angular frequency, $tg\delta$ is tangent of the dielectric loss angle, and u^* is the complex potential.

A linear variation of the electric potential inside each sub-domain *De* can be written as:

$$u_e(x,y) = \alpha_{e1} + \alpha_{e2}x + \alpha_{e3}y \text{ for e = 1,2,3,....} n_e \quad (11)$$

where $u_e(x,y)$ is the electric potential of any arbitrary point inside each-domain *De*, α_{e1}, α_{e2}, and α_{e3} reflect the computational coefficients for a triangle element *e*, n_e is the total number of triangle elements.

The calculation of the electric potential at every knot can be obtained as function *F(u):*

$$\frac{\partial F(u_i)}{\partial u_i} = 0 \text{ for } i = 1,2,\ldots\ldots n_p \quad (12)$$

Then, an equation of compact matrix can be obtained as:

$$[S_{ji}]\{u_i\} = \{T_j\} \text{ for } i,j = 1,2,\ldots\ldots n_p \quad (13)$$

where $[S_{ji}]$ is the coefficients matrix, $\{u_i\}$ is the unknown potential vector at the knots and $\{T_j\}$ is the free terms vector.

Magnetization Curve

Magnetization curve is related to magnetic field density (B) and magnetic field intensity (H). This curve shows the effect of magnetic field density, which occurs at the core of the transformer as a result of the increase in the intensity of the magnetic field.

Experimental Inrush Current Measurement

Experimental inrush current setup consists of the measurement phase and the demagnetization phase. The measurement phase is performed to obtain the value and waveform of inrush current. Demagnetization phase is performed after measurement phase. To obtain the value of inrush current that according to the initial condition when the transformer energized for the first time, the demagnetization process is required. Demagnetization method is performed using shunt capacitor and varying DC applied voltage with constant frequency.

A capacitor connected in parallel to the circuit has an effect in reducing the residual magnetism contained in the transformer [15]. While de-energizing, capacitive energy in capacitor can reduce inductive energy that contained in transformer. Three capacitors, which have a capacity of 400 μF 250 Volt are used in the experiment. Demagnetization circuit is shown in Figure 5.

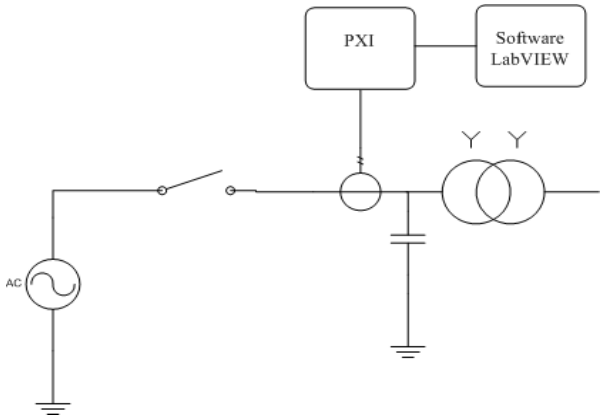

Figure 5. Demagnetization setup using shunt capacitor

By reducing the DC voltage magnitude successively every half cycle, the flux contained in the inductor will be gradually reduced every half cycle. The procedure begin by applying DC Voltage into the transformer until it reaches a saturated voltage, 380 VLL or 220 Vphase, then the voltage is reversed and reduced slowly. Frequency used in this circuit is 0.1 Hz. The concept of DC variable voltage-constant frequency obtained from study [16]. Figure 6 describes a circuit of this demagnetization.

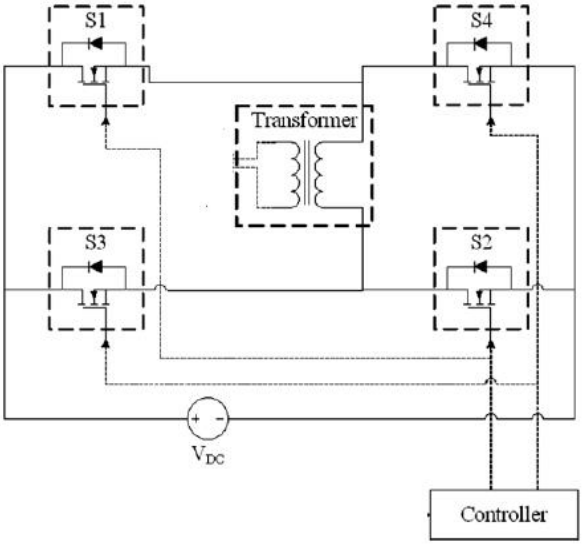

Figure 6. Variable voltage-constant frequency circuit

Analysis of Simulation and Experiment Result

Distribution of Magnetic Field Density (B) and Magnetic Field Intensity (H)

Figure 7 shows the results of 3D FEM simulation. From that figure, it can be clearly seen that the distribution pattern of the magnetic field density (B) of each transformer topology is different. The magnetic field density in type B is higher than type A. While the distribution of the magnetic field intensity (H) can be seen in Figure 8. Type B transformer also has higher magnetic field intensity rather than type A.

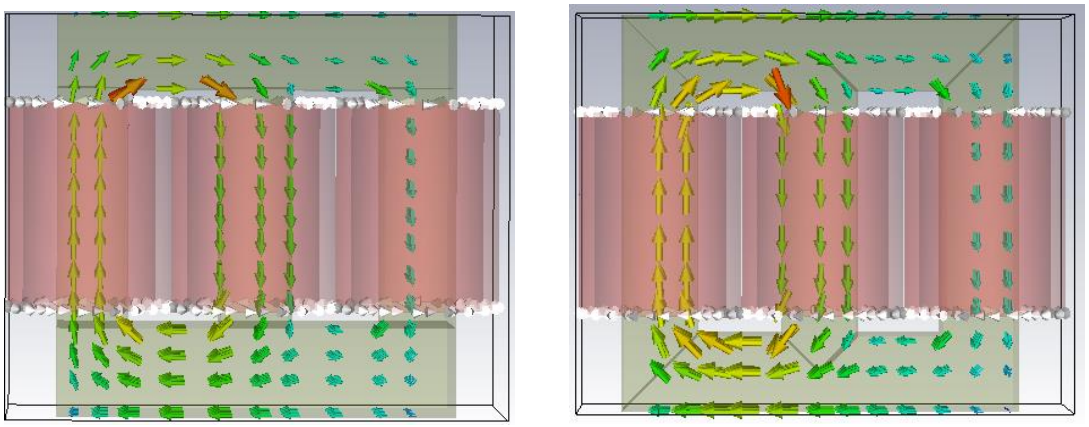

(a) (b)

Figure. 7. Distribution of the magnetic field density on phase 0^o; core cutting A (a), core cutting B (b)

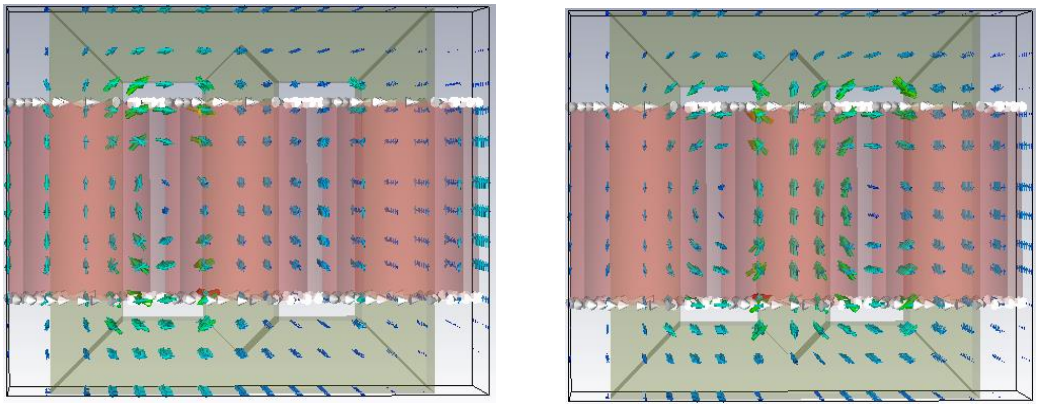

(a) (b)

Figure 8. Distribution of the magnetic field intensity by core cutting B on; phase 0^o (a), phase 120^o (b)

Magnetization Curves Comparison

Because the transformer core shape is continuous, observation of B and H value is performed at specific monitoring points. The monitoring points are applied on both transformers. Consideration in choosing these monitoring points is to observe the magnetization curves that occur in the joint part of transformer core cutting. Location of the monitoring points can be seen in Figure 9. Table 3 shows comparison of maximum magnetic field density magnitude. Figure 10, 11, and 12 represent magnetization curve characteristic comparison for core cutting A and B on different points. The comparison of magnetization curves for different core cutting results unique phenomena. The points at the jointing part have larger value of B and H than the points which are not located at the jointing part.

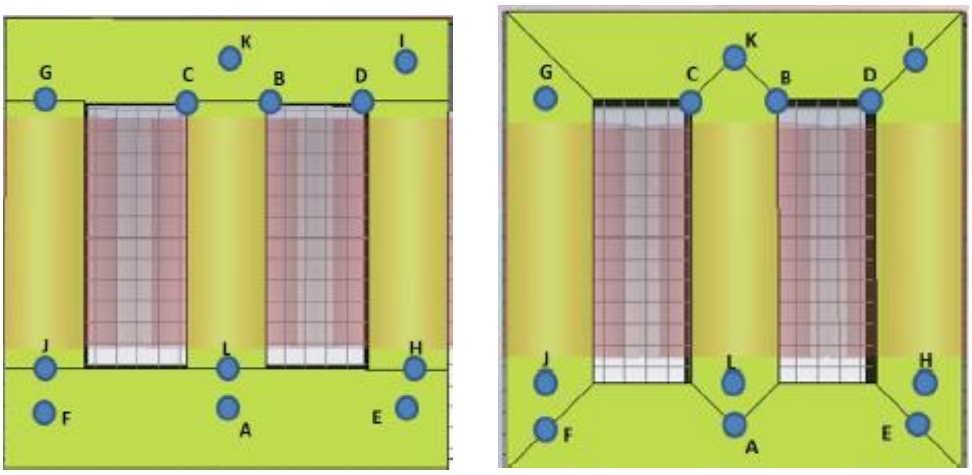

(a) (b)

Figure 9. Location of monitoring points at transformer core; cutting A (a), cutting B (b)

Table 3. Comparison Bmax Magnitude for Transformers

Monitoring Point	Magnitude of Maximum Magnetic Field Density (Vs/m^2)	
	Core cutting A	Core cutting B
A	0.89505311	1.854689467
B	1.298279302	1.744631571
C	0.733678361	1.813492198
D	0.023886761	0.505532615
E	1.646873892	1.558442573
F	0.743747092	1.179941983
G	0.962423258	0.864456119
H	0.105109613	0.145090947
I	0.639428183	1.357744277
J	0.664892251	0.030968433
K	1.663214618	1.32254227
L	0.450538411	0.230741026

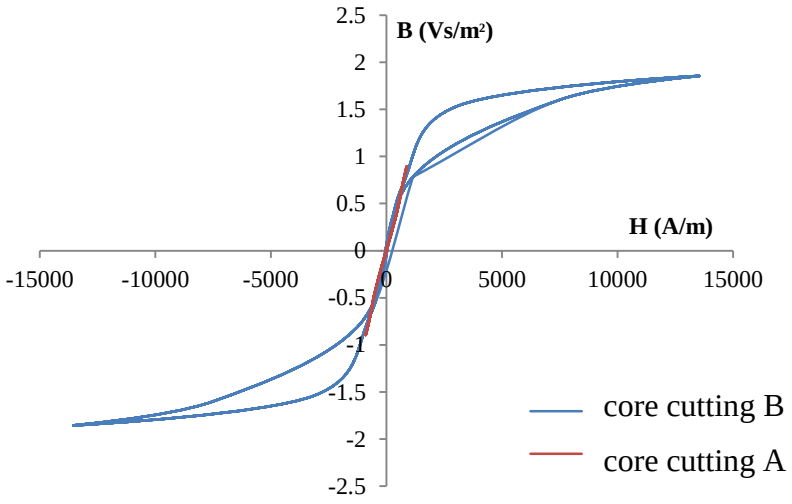

Figure 10. Comparison magnetization curve at point A

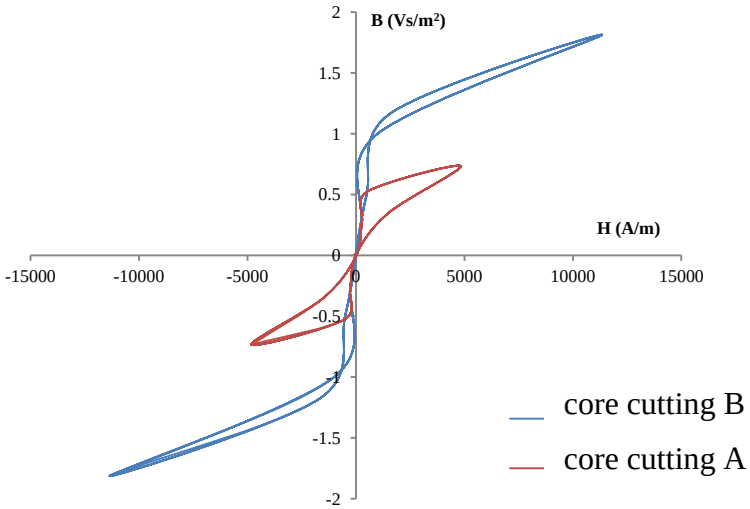

Figure 11. Comparison magnetization curve at point C

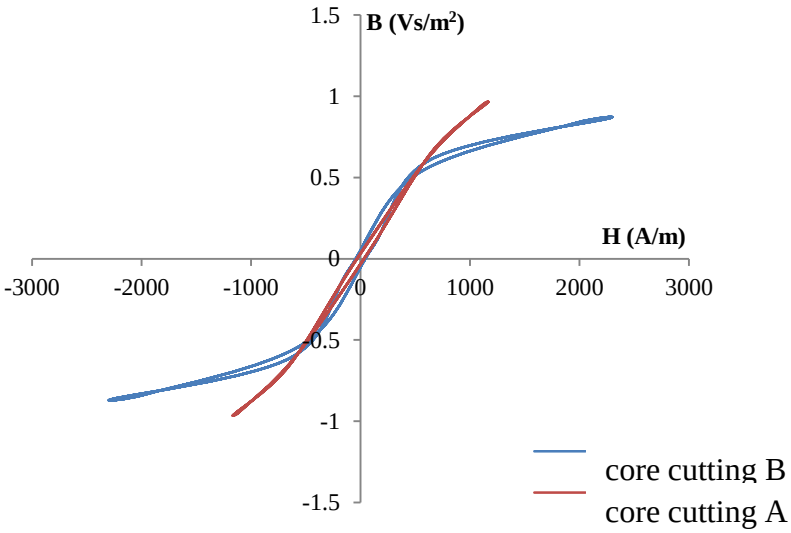

Figure 12. Comparison magnetization curve at point G

Effect of Transformer Core Cutting Topology on Inrush Current Peak Value Results of Simulation

Using Equation (4), the magnetization curve data can be processed to obtain inrush current. Results of inrush current calculation are resumed in Table 4. From that table, it can be seen that the maximum inrush current is 10.31 A at point E for core cutting A and 150.22 A at point A for core cutting B. The results show that the maximum inrush current is happened on different monitoring point.

Table 4. Calculation Approach of Inrush Current on Different Monitoring Points

Monitoring Point	Vm (Volt)	Maximum Inrush Current (A)	
		Core Cutting A	Core Cutting B
A	537.4	5.93	150.22
B	537.4	1.78	59.81
C	537.4	0.99	62.39
D	537.4	0.01	15.93
E	537.4	10.31	80.54
F	537.4	4.94	63.22
G	537.4	2.07	27.46
H	537.4	0.17	3.27
I	537.4	4.11	72.24
J	537.4	0.25	1.178
K	537.4	10.08	125.72
L	537.4	0.91	7.21

Experimental Result of Inrush Current Measurement

Inrush current magnitude of each transformer is compared on Table 5. The result show that core cutting B also has larger magnitude even it has different value with simulation result. Figure 13 show that measurement data has similar value of each day using shunt capacitor while Figure 14 are inrush current on each phase of the transformer. Those data show that transformer with core cutting B has larger magnitude than the transformer with core cutting A, although it has been demagnetized.

Table 5. Effect of Demagnetization on Inrush Current Magnitude

Effect of demagnetization	Inrush current (A)	
	Core cutting A	Core cutting B
Before demagnetization	13,2	>174
After demagnetization	11,2	174

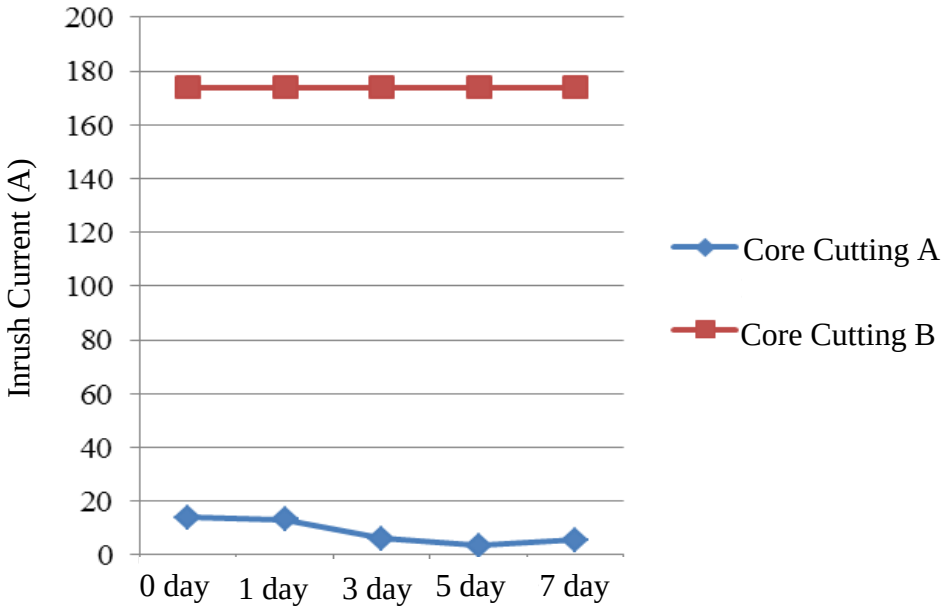

Figure 13. Inrush current magnitude after demagnetization using shunt capacitor in particular duration

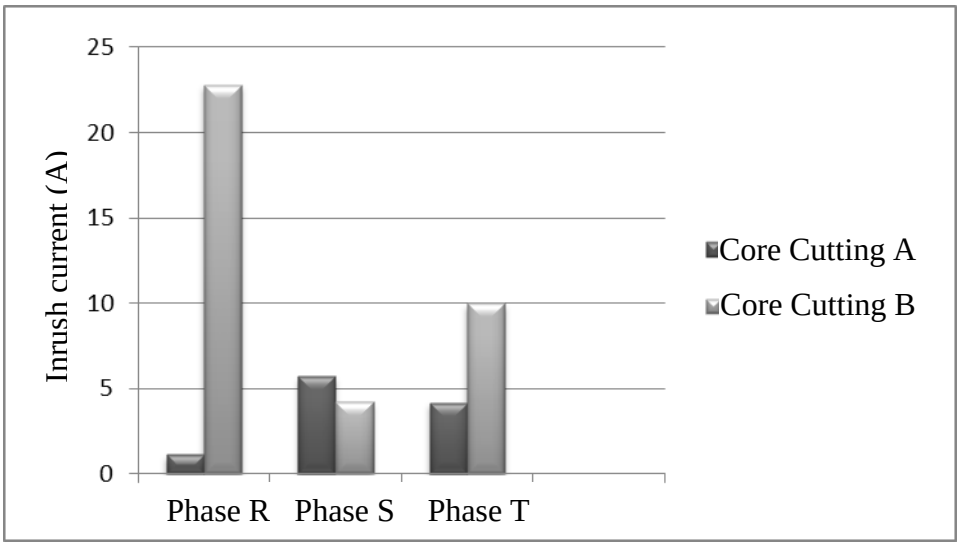

Figure 14. Inrush current magnitude on each phase after demagnetization using variable voltage – constant frequency

Physically the material used in transformer core cutting A seems cleaner and purer than core cutting B. Different element composed the core can affect value of material permeability. It causes the difference of B value. The high value of inrush current on transformer core cutting B indicates existence of large amount residual flux. This residual flux existence depends on transformer core magnetic properties. Furthermore, compactness of laminations and core cuttings also affect construction of core joint. Transformer core

cutting A is compacter than core cutting B. Thus air gap on core joint transformer B larger than transformer A. This fact also makes transformer B having louder buzz sound than transformer A and results higher inrush current magnitude. Moreover, Transformers used in the experiments was produced by different maker therefore we suggest that the material used was not similar.

Conclusions

In this study, effect of core cutting topology of transformer has been simulated and verified using experimental approach. The difference in magnitude and direction of the magnetic field distribution between core cutting A and core cutting B cause different characteristic of magnetization curves which has been proven by monitoring different point. In fact the magnetization curve was also affected by core material. This resulted in inrush current magnitude. The study shows that core cutting B has larger inrush current than core cutting A. Moreover, demagnetization method using the shunt capacitor and the variable voltage - constant frequency is also used to reduce the inrush current value. Meanwhile, the demagnetization does not change the fact that core cutting has effect on inrush current magnitude.

References

[1] S.J. Chapman, *Electric Machinery Fundamentals,* 4th Edition, McGraw-Hill Higher Education, New York, 2005.

[2] C.E. Lin, C.L. Cheng, C.L. Huang, and J.C. Yeh, "Investigation of magnetizing inrush current in transformers. II. Harmonic analysis," *IEEE Transactions on Power Delivery*, Vol. 8, No. 1, pp. 255-263, 1993.

[3] C.E. Lin, C.L. Cheng, C.L. Huang, and J.C. Yeh, "Investigation of magnetizing inrush current in transformers. I. Numerical simulation," *IEEE Transactions on Power Delivery*, Vol. 8, No. 1, pp. 246-254, 1993.

[4] K. Yabe, "Power differential method for discrimination between fault and magnetizing inrush current in transformers," *IEEE Transactions on Power Delivery*, Vol. 12, No. 3, pp. 1109-1118, 1997.

[5] P.L. Mao, and R.K. Aggarwal, "A novel approach to the classification of the transient phenomena in power transformers using combined wavelet transform and neural network," *IEEE Transactions on Power Delivery*, Vol. 16, No. 4, pp. 654-660, 2001.

[6] J.J. Rico, E. Acha, and M. Madrigal, "The study of inrush current phenomenon using operational matrices," *IEEE Transactions on Power Delivery*, Vol. 16, No. 2, pp. 231-237, 2001.

[7] A.A. Adly, "Computation of inrush current forces on transformer windings," *IEEE Transactions on Magnetics*, Vol. 37, No. 4, pp. 2855-2857, 2001.

[8] P.C.Y. Ling, and A. Basak, "Investigation of magnetizing inrush current in a single-phase transformer", *IEEE Transactions on Magnetics*, Vol. 24, No. 6, 1988.

[9] S.D. Chen, R.L. Lin, and C.K. Cheng, "Magnetizing inrush model of transformers based on structure parameters," *IEEE Transactions on Power Delivery*, Vol. 20, No. 3, 2005.

[10] P.S. Moses, M.A.S. Masoum, and M. Moghbel, "Effects of iron-core topology on inrush currents in three-phase multi- leg power transformers," Paper presented at *2012 IEEE Power and Energy Society General Meeting*, United States of America, 2012.

[11] M. Khelil, and M. Elleuch, "Modelling of the air-gaps of overlapped joints in tree-phase transformer iron core for using by FEM," Paper presented at the *6th International Multi-Conference on Systems, Signal and Devices*, Tunisia, 2009.

[12] B. Arif. *Pengaruh Cara Pemotongan Inti Transformator Terhadap Kurva Magnetisasi Dan Inrush Current, Institut Teknologi Sepuluh Nopember*, Surabaya, 2015.

[13] I.M. Yulistya Negara, Dimas A. Asfani, D. Fahmi, S. Baskoro, and B. Arief, "Material and cutting method effects of three phase transformer-core on magnetization curve and inrush current: Simulation approach," *International Review on Modelling and Simulations (IREMOS),* Vol. 8, No. 3, 2015.

[14] M. Jamali, M. Mirzaie, and S.A. Gholamian, "Calculation and analysis of transformer inrush current based on parameters of transformer and operating conditions," *Electronics and Electrical Engineering*, No. 3, 2011.

[15] B. Kovan, F. de León, D. Czarkowski, and L. Birenbaum, "Mitigation of inrush currents in network transformers by reducing the residual flux with an ultra-low-frequency power source," *IEEE Transactions On Power Delivery,* Vol. 26, No. 3, 2011.